Time Varying Nonlinear Schrödinger Equation: Bose-Einstein Condensation via Gross-Pitaevskii Eq.

A. J. Kalinowski*[1]
[1]Consultant
*Corresponding author: East Lyme CT 06333, kalinoaj@aol.com

Abstract: COMSOL is used for obtaining the quantum mechanics wavefunction Ψ(x,y,z,t) as a solution to the *time dependent* nonlinear Schrödinger equation (NLSE) representing a typical (near absolute zero) boson particle (while it interacts with N like neighboring particles). The additional nonlinear term in the usual linear Schrödinger equation is caused by interactions with the contiguous boson particles. The probability density evaluation of a particle being at a spatial point can be obtained from $|\Psi|^2$. Numerical solutions to NLSE are sought herein and because it involves solving field PDEs, COMSOL is directly adaptable to the problem at hand.

Keywords: Quantum Mechanics, Time Dependent Schrödinger Equation, Wave Propagation.

1. Introduction

The paper illustrates the use of COMSOL for obtaining the solution Ψ(x,y,t) as a solution to the *time dependent nonlinear* Schrödinger equation (NLSE). COMSOL has been used to solve the time dependent *linear* Schrödinger equation in Ref.[1], however this is the first application to the NLSE . The words "Schrödinger equation" is usually associated with quantum mechanics, however in the case of the nonlinear version, there are a wide variety of other applications well outside the realm of quantum mechanics. The NLSE appears in several branches of physics such as a) the quantum physics Bose-Einstein condensation (BEC) where it is represented via the Gross-Pitaevskii equation (GPE), b) laser beam propagation in nonlinear quantum optics, c)ocean time varying gravity-capillary surface waves, d) plasma and particle physics, e) semiconductor applications, f) first principle material simulation, g) superfluids, and h) biological molecular systems where references for all of these are found in Ref.[2]. The (a) GPE example is selected as the one examined in this paper. This is perhaps the most complicated all of the examples, because it contains an additional V(x,y) potential term (proportional to Ψ(x,y,t)) in the governing PDE. The quantum mechanics wavefunction Ψ(x,y,z,t) is sought which represents the behavior of a typical (near absolute zero temperature) boson particle (while it interacts with N like neighboring particles found in a dilute gas of bosons that are all in the same quantum ground state). The additional nonlinear term $\Psi\beta|\Psi|^2$ appearing in the usual linear Schrödinger equation, is caused by interactions with the contiguous boson particles.

2. Governing Equations/Theory

2.1 2-D time dependent NLSE

The governing non-dimensional 2-D version of the GPE equation for the Ψ(x,y,t) behavior of a representative boson particle in a extremely cold dilute gas of N particles in non-dimensional form is given by Ref.[3]:

$$i\frac{\partial\Psi}{\partial t} = -\frac{1}{2}\left(\frac{\partial^2\Psi}{\partial x^2}+\frac{\partial^2\Psi}{\partial y^2}\right) + \Psi\{V(x,y)+\beta f(\Psi)\} \quad (1)$$

$$V(x,y) = \alpha\frac{1}{2}\left(\gamma_x^2(x-x_o)^2 + \gamma_y^2(y-y_o)^2\right) \quad (2)$$

$$f(\Psi) = |\Psi|^2 \quad (3)$$

where V(x,y) in Eq.(3) is an external trapping potential (with unit-less strength parameters γ_x , γ_y and sign multiplier $\alpha = \pm 1$ (with plus 1 corresponding to a confining potential or minus 1 corresponding to an attractive potential e.g. Ref. [2]); β is a unit-less interaction parameter that is proportional to N (with positive for repulsive interaction and negative for attractive interaction e.g. Ref.[2]) ; $\{x_o,y_o\}$are offset distances setting the start of the potential and $i=\sqrt{-1}$. The Eqs.(1-3) "Times font" variables Ψ,t,x,y are in non-dimensional form and can be related back to the "Chalkduster font" dimensional variables Ψ,𝔱,𝔵,𝔶,ω by Ref.[3]: $t=\omega_m\mathfrak{t}$, $x=\mathfrak{x}/a_o$, $y=\mathfrak{y}/a_o$, $\Psi(x,y,t)= (a_o)^{3/2}\Psi(\mathfrak{x},\mathfrak{y},\mathfrak{t})$, $\omega=\omega/\omega_m$ with harmonic oscillator ground state length $a_o=\sqrt{(\hbar/(m\omega_m)}$ where ω_m=minimum trap frequency, $\hbar$=Planck's constant, m=boson atomic mass and ω=dimensional drive

frequency used later as time harmonic drivers in the FEM models. Refer to Ref.[2] for details on selecting the γ_x , γ_y , β parameters.

2.2 *1-D PW Local k-ω Dispersion Relation*

The governing non-dimensional 1-D version of the local PDE (i.e. temporarily holding independent variables {x=x′, y=0} constant in the Eq.(2) V(x′)) for the Ψ wavefunction will be useful in predetermining an estimated effect of the potential on an otherwise propagating free field PW wavefunction. Start by assuming a PW solution of the form :

$$\Psi(x,y,t) = \psi_o\, e^{ikx - i\omega t} \qquad (4)$$

and substituting this into Eqs.(1-3) yielding:

$$k_s = \pm\sqrt{2\omega - (\,\alpha\gamma_x^2(x'-x_o)^2 + \beta|\psi_o|^2\,)} \qquad (5)$$

$$\lambda_s \equiv real\ pt\,(2\pi/k_s) \quad \overline{\lambda} \equiv \lambda_s/\lambda_{FF} = \lambda_s/(\pi/\sqrt{\omega/2}) \qquad (6)$$

The $\overline{\lambda}$ variable is the normalized λ_s (by the free field Schrödinger PW wave length $\lambda_{FF} = \pi/\sqrt{(\omega/2)}$) and is used in later $\overline{\lambda}$ vs x plots. The V(x) coefficient in Eq.(1) actually varies with x so a typical algebraic k-ω dispersion relation is not possible, therefore the next best thing is getting an Eq.(5) local steady state solution k_s valid in the neighborhood of x=x′. Consider the x′ neighborhood region $x'-\varepsilon\lambda_s \le x \le x'+\varepsilon\lambda_s$, where $\pm\varepsilon\lambda_s$ is the width to either side of x′ in terms of an ε fraction of the steady state wave length λ_s (e.g. ε=1/4 implies $2\varepsilon\lambda_s$ spans 1/2 wave length). The following Eq.[7] relation:

$$\mathcal{R} \equiv \frac{V(x'+\varepsilon\lambda_s) - V(x'-\varepsilon\lambda_s)}{V(x')} = \frac{4\varepsilon\lambda_s}{(x'-x_o)} \qquad (7)$$

gives a measure (i.e. a central difference ratio R) of how variable V(x) is over the range $2\varepsilon\lambda_s$ surrounding x′. For instance in a later Fig.(2) example, using Eqs.(5-6) gives a predicted wave length λ_s = 0.415 at x′=34.7 and with x_o=18.5 and ε=1/4, Eq.[7] gives $\mathcal{R}$=0.0256 which implies V(x) deviated from being constant by only 2.56 % over a 1/2 wave length span.

Finally, it is noted that unlike k-ω dispersion relations derived from linear PDE's, the one derived from our Eq.(1) nonlinear PDE contains the ψ_o PW amplitude as part of the dispersion relation. Note also that when parameters γ_x , β parameters are set to zero, the usual Schrödinger equation dispersion relation is recovered.

The k_s wave number approximation is used for the following reasons: (1) for harmonically driven problems solved later, obtain an estimate of the Ψ spatial wave length (via Eq.(6)), for use in FEM mesh size selection (2) used to compute a PW boundary condition absorber where applicable.

3. Method

A Bose-Einstein condensation domain is interfaced with a neighboring free field startup domain (i.e. with the γ_x , γ_y , β parameters turned off). A free field harmonic PW of prescribed drive frequency ω passes through the startup zone and encounters the Bose-Einstein condensation zone. The transition between the free field domain and the BEC domain is in a accomplished by multiplying COMSOL's "*STEP* function H(x-x_o)" (with gradual cubic ∫ shaped transition rise over width Δx_t) times the γ^2_x , γ^2_y , β terms inside the brace { } terms appearing in Eq.(1). The NLSE equation is solved in the time domain (using the General-Form PDE "time dependent" module) by driving an upfield face of a model (initially at a zero wavefunction state) with exp(-iωt) harmonic loadings, and then track the transient wave that propagates towards the downfield model's end.

3.1 FEM Boundary Conditions

3.1.1 FEM Wave Generation Driven Surface: transient solutions are generated by driving the upfield surfaces with time harmonic loadings at frequency ω of the form:

$$\Psi(x_s,y_s,t) = \psi(x_s,y_s)\,F(t)\,e^{-i\omega t} \qquad (8)$$

where $F(t)$ is a gradual time increasing multiplier on the harmonic driver and $\psi(x_s,y_s)$ is the wavefunction distribution (e.g. from a free field PW) at surface points $\{x_s,y_s\}$. This gradual increase is to help minimize any suddenly applied loading effects (e.g. for the front end of driver):

Firstly in $F(t)$, the [ ] bracket term in first of Eqs. (9) exponentially increases from ε_0 to 1.0 over startup N_c time cycles. Using transition term $U_2(t)$, the starting value, $F(0)= \varepsilon_0$, is made zero by:

$$F(t) = U_2(t)\,[\,U_3(t) + U_4(t)\exp(\eta(\,t - t_c))\,] \qquad (9)$$

$$U_3(t) = 0 \;\; t < t_c \;;\; = 1/2 \;\; t = t_c \;;\; = 1 \;\; t > t_c$$

$$U_4(t) = 1 \;\; t < t_c \;;\; = 1/2 \;\; t = t_c \;;\; = 0 \;\; t > t_c$$

$$U_2(t) = 0 \;\; t < 0 \;\; ; = 2\frac{t^2}{t_w^{\,2}}\left[\frac{3}{2} - \frac{t}{t_w}\right] \;\; 0 \le t \le t_w \;;$$

$$= 1 \;\; t > t_w$$

$$t_c = \frac{2\pi N_c}{\omega};\; \eta = \frac{-\ln(\varepsilon_0)}{t_c};\; N_c = 3;\; \varepsilon_0 = .05;\; t_w = .1$$

blending $F(0)$=0 into $F(t_w)$ with a cubic ∫ *shaped* curve ending at t=t_w . The $\Psi(x_s,y_s,t)$ input driver, using the Eqs.(9) Nc, ε_0 , t_w parameters@ ω=15,

is shown in Fig.(1a) for an infinite wave train. Figure(1b) shows the FFT of the real part of the Ψ driver where a dominant spike is at the drive frequency ω=15 .

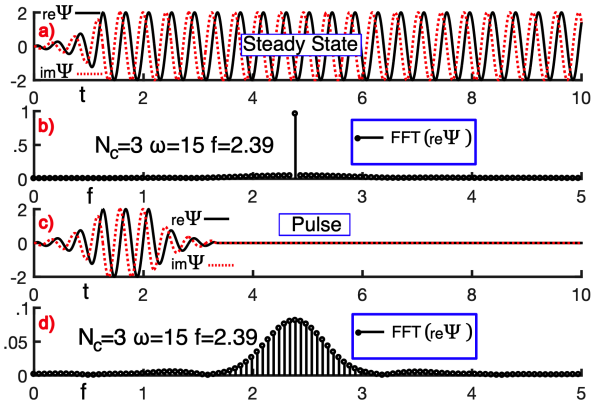

Figure 1. Wave Train vs Pulse $\Psi(x_s,y_s)$ Driver

The $\Psi(x_s,y_s,t)$ input driver, using the same parameters, is shown in Fig.(1c) for a pulse having the same Nc=3 front end as in Fig.(1a), followed by 2 flat cycles followed by a reverse exponential 3 cycle coast down similar to the front end build up. The non-spiked FFT amplitude spread in Fig.(1d) centered about the drive freq. suggest that other harmonics might be excited for pulse drive models.

3.1.2 FEM Model BC Termination Surfaces:

(i) absorbing BC: simple $\vec{n}\bullet\vec{\nabla}\Psi(x_b,y_b,t)=ik_s\Psi$ PW absorbers are used when traveling waves impinge on the FEM model when applicable, otherwise the computations are halted before the wave hits the boundary.

(ii) zero value BC : for waves that never reach the outer mesh, this is used down field of the propagation at the outer boundary points $\{x_b,y_b\}$ of the model, namely $\Psi(x_b,y_b,t)=0$

(iii) normal gradient BC: normal grad. $\vec{n}\bullet\vec{\nabla}\Psi(x_b,y_b,t)=0$, @ surface points $\{x_b,y_b\}$, where $\vec{n}$ is a surface unit normal vector (used while solving Eq.(1) at wave guide y=constant cuts).

3.2 FEM Initial Conditions

The FEM model is started from rest throughout the entire spatial domain $\mathcal{D}$, therefore: $\Psi(x_s,y_s,0)=0$.

Because of the manner Eq.(9) is constructed, evaluating it at t=0 is consistent with $\Psi(x_s,y_s,0)=0$.

3.3 Model Parameters

The physical parameters in the PDE coefficients of Eq.(1) (β, $\alpha\gamma^2_x$, $\alpha\gamma^2_y$) are swept over a ± range of values and are indicated for each example problem solved. In all models the same non-dimensional drive frequency ω=15 was used as well as the driver amplitude $\psi(x_s,y_s)=\psi_o=2$.

4. Nonlinear Schrödinger Equation Results for GPE

Exact Eq.(1) validation solutions to wave propagation problems (when the V(x) potential is present) are not generally possible, even for simple 1-D propagation. Instead COMSOL comparisons to the same problem solved by an alternate FEM code (e.g. Mathematica™) is made. The intent here is to exercise COMSOL through a varied combination of model parameters (i.e. ±V, ± β) and observe how the resulting solutions are effected by these variations and how they compare to the alternate FEM solver.

4.1 Bar PW Wave Guide in a V(x) Potential Field

4.1.1 Ψ Wave Train Sol. : γ_x=1 , β=10 , α= -1 :

A Fig.(2a) inset WxL=.4x70 FEM 2-D bar with *attractive V potential* (i.e. α = -1) and *repulsive NL (NonLinear) interaction* (i.e. β>0) is driven via Eqs. (8-9) on the upfield end surface by a uniform loading with the Fig.(1a) wave train driver @ N_c=3) while using the (ω, ψ_o) **3.3** model parameters. This bar example and

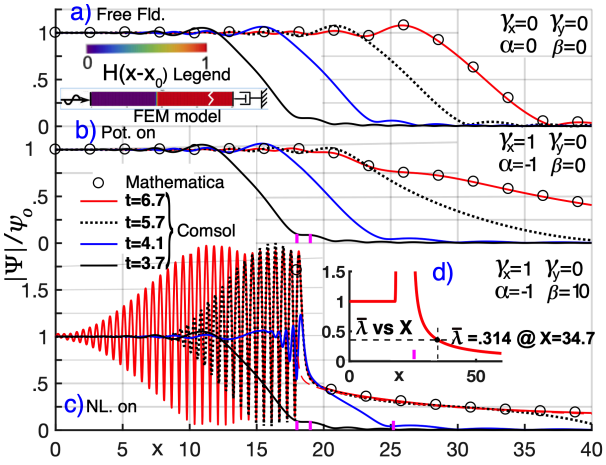

Figure 2. Ψ vs x,t for Wave Train Sol. γ_x=1, β=10, α= -1

all subsequent 1-D ones, use 2-D quadratic finite elements even though 1-D elements would be sufficient (want to test the quality of the quad element performance for later use in actual section **4.2** 2-D models). The color coded FEM model plot shows the point at which the H(x-xo) turns on with ∫ shaped step transition distribution over Δx=1 (where in COMSOL xo= 18+Δx/2=18.5 is at the center of the transition). Further the transition zone is denoted by the first and second pink tick marks at x=18,19 in Figs(2b-c). The Fig.(2d) $\bar{\lambda}$ *vs* x via Eq. (6), shows that local NL steady state waves are possible for x> 25.2 (3d Fig.(2c) and 1st Fig.(2d) pink tick marks). The gap between 18<x<25.2 in the Fig.(2d) plot, is where there is no real root to Eq.(5), however it is still possible to send a non-

harmonic signal through the gap. The solutions to Eq.(3) are displayed as the $|\Psi|/\psi_o$ vs x for a sequence of 4 fixed time values. The Figs.(2a-c) shows the effect of (a) V Potential and NL β term turned off, (b) turning on only the V potential, and (c) both potential V and NL β terms turned on for a sequence of 4 successive time values. There is good comparison between the COMSOL and Mathematica™ solutions at the last time value t=6.7 . Note that as each V, β component is turned on in the Eq.(3) PDE, the slope of the wave front vs x gets flatter compared to the Fig.(2a) free field case. There are strong reflections from the portion of the PDE (wave entrance thru the transition zone) when the NL β term is in play. The corresponding normalized $\Psi(x)/\pi$ phase rolloff (in radians) at t=6.7 is shown in the left half of Fig. (4a-c). The repeated $\Psi(x)/\pi$ phase pattern of -1 to +1 indicates a traveling wave, where comparisons of COMSOL to Mathematica results are good. The λ_G=0.36 graphically measured wave length at x=34.7 (e.g. see Fig.(4c)), is compared to the λ_s = 0.415 predicted value from the 1st of Eq.(6), (e.g. Fig.(2d) *normalized* $\bar{\lambda}$ =0.314 via 3d Eq.(6)) which corresponds to a 13% difference between λ_G and λ_s . This illustrates that the prediction is good enough to size the number of FEM elements per wave length for use in the quadratic elements. The value of k_s can also be used to size PW absorbers via $\partial\Psi/\partial x = i\, k_s \Psi$ while evaluating k_s at x′=L (the end of the FEM model). A wave guide side wall $\partial\Psi/\partial y=0$ BC is used on this and all later 1-D models.

4.1.2 Ψ Pulse Sol. : γ_x=1 , β=10 , α= -1 :
This Fig.(3) is a repeat of the previous 4.1.1 example, except the loading is the Fig.(1c) pulse driver.

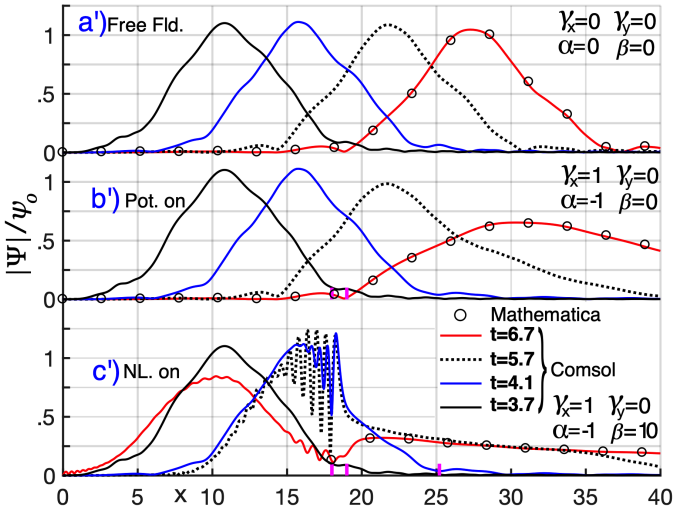

Figure 3 Ψ vs x,t for Pulse Sol. γ_x=1, β=10, α= -1

The corresponding phase roll off is shown in the right half of Fig.(4a′-c′). Again there is good agreement between Mathematica™ and COMSOL. Comparing plots a′,b′,c′ of Fig.(3), the pulse shape distortion caused by turning on each term in the PDE is clearly illustrated (e.g. the dispersion effect of the potential V(x) term spreads out the snapshot of the pulse shape at each increasing time value plotted). The pulse cuts the tail time loading duration, therefore there is less back scattering off the transition zone.

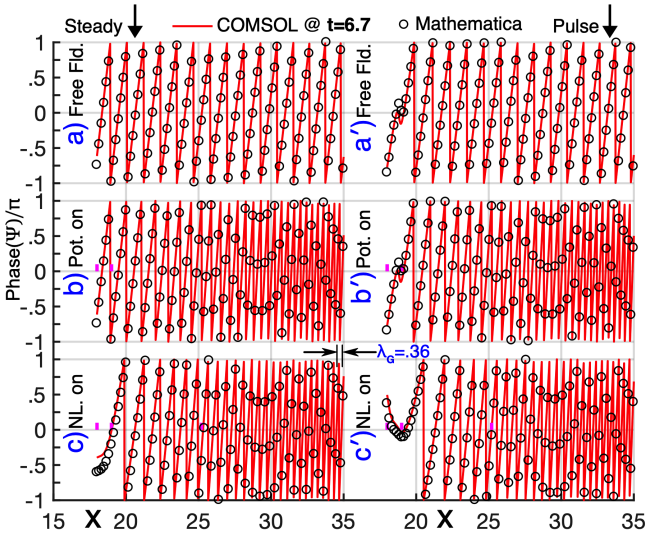

Figure 4 Ψ Phase vs x for Pulse Sol. γ_x=1, β=10, α= -1

4.1.3 Ψ Wave Train Sol. : γ_x=1 , β=10 , α= +1 :
This is a repeat of 4.1.1, except for a *confining potential V* (only differences are α= +1, a shorted model L=40 and fixed termination BC). Equation (6)

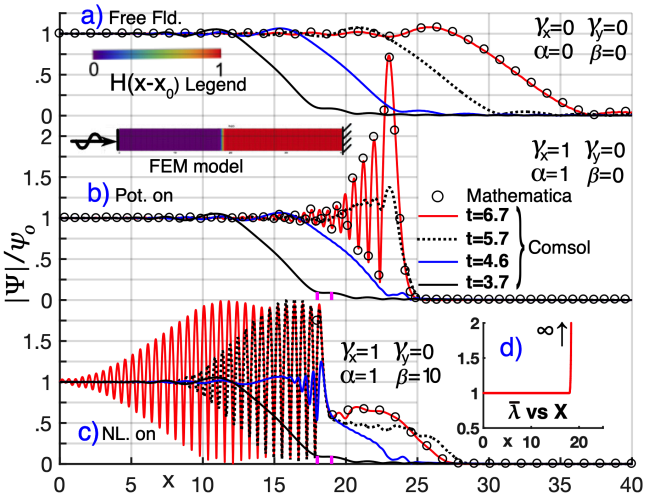

Figure 5 Ψ vs x,t for Train Sol. γ_x=1, β=10, α= +1

predicts (e.g. Fig.(5d) inset) no harmonic waves beyond the transition zone (e.g. Fig.(5b-c) pink tic markers) as seen in Fig.(5c), where |Ψ| stalls out around x=28 as compared to Fig.(2c), where the wave proceeds well past this x point.

4.1.4 Ψ Pulse Sol. : γ_x=1 , β=10 , α= +1 :
This is a repeat of the previous 4.1.3 example, except here the loading is the Fig.(1c) pulse driver. The corresponding numerical solution is given as:

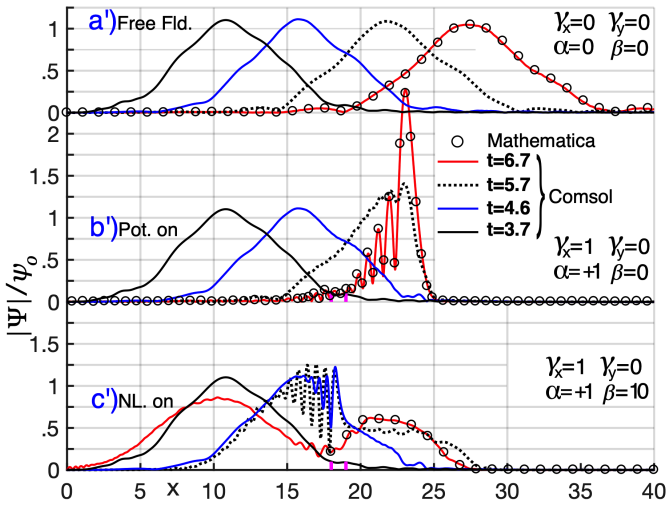

Figure 6 Ψ vs x,t for Pulse Sol. γ_x=1, β=10, α= +1

where again it is noted that the |Ψ| stalls out around x=28 in the x′ direction as compared to Fig. (3c), where the wave proceeds past this x point.

4.1.5 Ψ Wave Train Sol. : γ_x=1 , β= -10 , α= -1 :
A WxL=.4x70 FEM 2-D bar with *attractive V potential* (i.e. α = -1) and *attractive NL interaction* (i.e. β<0) is driven with the Fig.(1a) wave train driver.

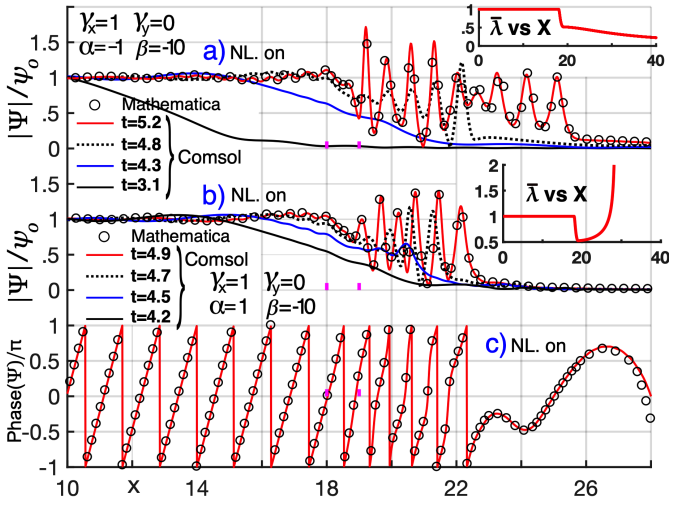

Figure 7 |Ψ| vs x,t for Wave Train Sol. γ_x=1, β=-10, α=±1

Due to space limits, this example and the 4.1.6 next one, display only the full wave train solutions without the effect of sequentially turning on the PDE's separate terms. The Fig.(7a) inset, for local wave length prediction plot, indicates a positive real $\bar{\lambda}$ vs x over the length of the model and therefore the model is terminated with a PW absorber. The t=5.2 behavior of |Ψ| looks unusual in the range starting at the end of the transition zone (pink tic markers) and ending at around x=25.8, wherein the 9 distinct peaks resemble a standing wave pattern. The remaining x>25.8 curve portion turns into a downward sloping flat plot similar to the Fig.(2c) example.

4.1.6 Ψ Wave Train Sol. : γ_x=1 , β= -10 , α= -1 :
A WxL=.4x40 FEM 2-D bar with *confining V potential* (i.e. α = +1) and *attractive NL interaction* (i.e. β<0) is driven with the Fig.(1a) wave train driver. The Fig.(7b) inset, for local wave length prediction plot, indicates a positive real $\bar{\lambda}$ vs x only up to asymptotic value x= 28.1 and therefore no traveling waves are expected to reach the end of the model and thus a simple Ψ=0 terminated BC is used. Again the t=4.9 behavior of |Ψ| looks unusual in the range starting at the end of the transition zone (pink tic markers) but here ending at around x=23, wherein the 6 distinct peaks resemble a standing wave pattern. The remaining x>23 curve portion turns into a shallow downward sloping flat plot → 0 , similar to the Fig.(5c) example. Finally Fig. (7c) illustrates the t=4.9 unusual phase roll off once past the transition zone (pink tics) (also experienced by Mathematica™).

. 4.2 PW thru 2 Slits into a V(r) Potential Field

The 2-D counterpart of 4.1 is treated by passing a PW through two A_p=1/2 aperture slits (separated by pitch P=5) into a R=30 semicircular zone with a $0 \le r = \sqrt{(x^2+y^2)} \le r_o$ start up free field zone (i.e. V=0 and β=0) followed by a spatially gradual turned on V and β over Fig.(8a) dashed zones $r_o \le r \le r_o + \Delta r$) using COMSOL's cubic ∫ shaped step function centered at $r_o + \Delta r/2$ with r_o=3 & Δr=1.

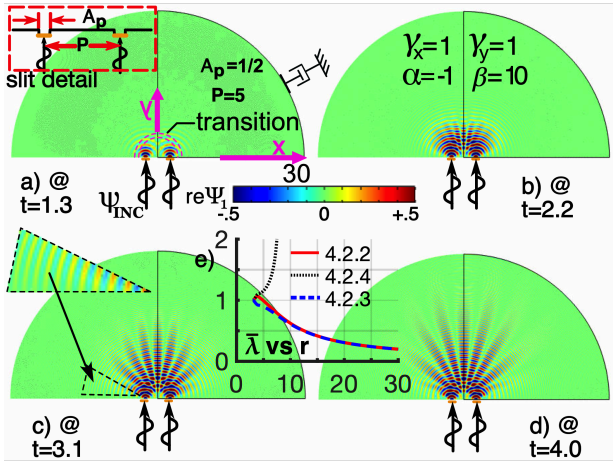

Figure 8 reΨ for 2 Slit Sol. $\gamma_x = \gamma_y$=1, β=10, α= - 1

Enlarging the Fig.(8a) source region would reveal the bounding pink dashed transition zone. The open slit faces are driven with the Fig.(1a) train of wave input, where the remaining horizontal boundary containing the slit uses a $\Psi(x_b,y_b,t)=0$ BC . The outer circular arc surface uses a CylW absorbing BC when outward radial waves are expected and a $\Psi(r=R,t)=0$ BC when outward waves can't reach the boundary in accordance with the prediction made by the local wave length calculation (e.g. curve labeled 4.2.4 in Fig.(8e)).

4.2.1 1-D CylW Local k-ω Dispersion Relation: Figure(8a) displays cylindrical shaped waves emanating from each slit before interaction. Therefore it is of interest to modify Eq.(5) for out going cylindrical waves fields, where the following 4 steps are made: 1) express Eq.(1) in (r,θ) cylindrical coordinates with no θ dependence; 2) hold r=r′ constant in the { } Ψ coefficient; 3) restrict $\gamma_x = \gamma_y \equiv \gamma_r$; 4) for sufficiently large kr arguments, use $Aexp(i(kr-\omega t)/\sqrt{r}$ as an approximate cylindrical coordinate solution to Eq. (1) (where the approximation $\nabla^2(\Psi) = [-1+1/4(kr)^2]k^2Aexp(i(kr-\omega t)/\sqrt{r} \approx -k^2Aexp(i(kr-\omega t)/\sqrt{r}$ is made dropping H.O.T. $1/4(kr)^2$]). The constant $A \equiv \Psi_{Ro}/\sqrt{(1/R_o)}$ is selected so $\Psi = \Psi_{Ro}$ at wave starting radius $r=R_o$. Applying conditions 1-4, and substituting $Aexp(i(kr-\omega t)/\sqrt{r}$ into the cylindrical coordinate form of Eq.(1), results in following k-ω expression.

$$k_s = \pm\sqrt{2\omega - \{\alpha\gamma_r^2(r'-R_o)^2 + \beta\left|\psi_{R_o}/\sqrt{(r'/R_o)}\right|^2\}} \qquad (10)$$

Ψ_{Ro} is set as the starting potential value at starting radius R_o (e.g. in section 4.2.2 example, $\Psi_{Ro} \approx 0.5$ at R_o=3.5 where the 0.5 value is read off free field radiating cyl. wave Fig.(11a) at r=3.5).The local wavelength $\bar{\lambda}$ vs r plots using (Eq.(10) with Eq.(6) for the 3 examples to follow) are shown in Fig.(8e) .

4.2.2 Ψ Wave Train Sol. : $\gamma_x=\gamma_y=1$, $\beta=10$, $\alpha=-1$: A 4 time snapshot sequence of the evolution of the Re *pt* Ψ(x,y,t) is shown in Fig.(8a-d), where the evolution of interference patterns is shown. The solid red local wavelength $\bar{\lambda}$ vs r plot labeled 4.2.2 shown in Fig. (8e), predicts traveling waves are possible and at a decreasing wavelength (e.g. Fig.(8c) triangular cutout enlargement) in the direction of propagation. The corresponding |Ψ(x,y,t)| field @t=4 is shown in Fig.(9c), (note that |Ψ(x,y,t)| is related to the quantum mechanics probability density $\rho(x,y,t) \equiv |\Psi(x,y,t)|^2$). A cut labeled C-C @ y=10 through the Fig.(9c) result is shown in Fig.(10c), where the resulting red curve constructive and destructive interference pattern is illustrated by the alternating peak-valley-peak pattern. The comparative reference solution of the free field Schrödinger equation (i.e. no V(x,y) potential and no nonlinear β term) is illustrated in Fig.(9a) for the |Ψ(x,y,t)| field plot, and in Fig.(10a) as the red interference pattern. The consequence of the γ_x , γ_y , β parameters turned on in Figs.(10b→d) is that the seven interference peaks are lower and also shifted for the six off center ones.

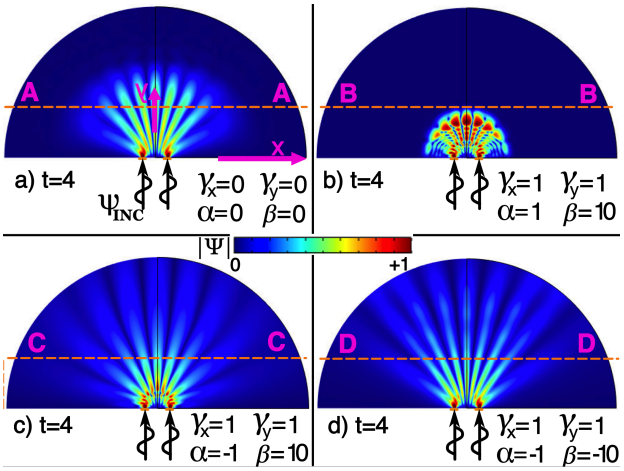

Figure 9 |Ψ | vs x,y for Linear vs Nonlinear 2 Slit Sol.

4.2.3 Ψ Wave Train Sol. : $\gamma_x=\gamma_y=1$, $\beta=-10$, $\alpha=-1$: This is the same as the previous 4.2.2 example, except that the nonlinear term has a positive β coefficient. The solid red vs dashed blue local wavelength $\bar{\lambda}$ vs r plot shown in Fig.(8e), illustrates that for r>10, the traveling wave predictions are essentially the same. The |Ψ(x,y,t)| field is shown in Fig.(9d), and the associated interference curves in Fig.(10d), where the width, of the constructive interference radial spikes (@ β= -10) are narrower and longer than the previous 4.2.2 (@ β=+10) example.

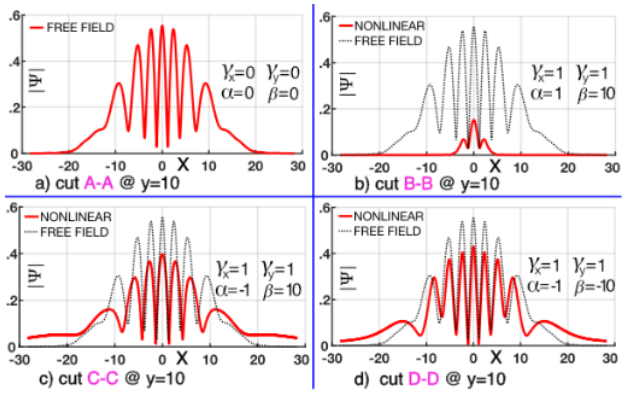

Figure 10 |Ψ | vs x at y=constant Interference Pattern

4.2.4 Ψ Wave Train Sol. : $\gamma_x=\gamma_y=1$, $\beta=10$, $\alpha=1$: This is unlike the previous 4.2.2 & 4.2.3 examples in that the entire { } brace coefficient in Eq.(10) stays positive and therefore as *r′* increases, it continues to over power the 2ω term resulting in no real values for $\bar{\lambda}$ beyond a cutoff radius

indicated by the black dotted $\bar{\lambda}$ vs r plot labeled 4.2.4 shown in Fig.(8e). The corresponding |Ψ(x,y,t)| field is shown in Fig.(9b), and associated interference curves in Fig.(10b), where as shown, the typical wave interference pattern associated with two superimposed traveling waves is not present.

4.3 PW thru 1 Slit into a V(r) Potential Field

This example is the same as **4.2**, except only one slit is present and the start of the transition radius surrounding the slit is smaller because only one slit needs to be surrounded with a free field zone (r_o =1).

4.3.1 Ψ Wave Train Solution :

The 1 slit |Ψ(x,y,t)| field solution counterpart to Fig.(9) is shown in Fig.(11) (where all problem parameters are kept the same). Only one cylindrical type wave emanates from the single slit, therefore no spoked alternating constructive and destructive interference patterns are expected. Upon comparing the NLSE wave propagation cases (i.e. Fig.(11c&d)) to the Fig. (11a) linear free field Schrödinger equation solution , it is observed that in the second radial half of the Fig. (11c&d) model (r>R/2), a light blue region surrounds the slit out to the boundary that is not present in the Fig.(11a) model. This (r>R/2) light blue region is in the Fig.(9c&d) two slit models as well. This farther reaching effect beyond the Schrödinger equation free field solution is also present in the simple 1-D PW models, where for example PW solution Fig.(2c) is the 1-D counterpart of 2-D two-slit Fig.(9c) and of the 2-D one-slit Fig.(11c). Focusing on the Fig.(2) |Ψ(x)| response @ x=40, when both the potential and nonlinear term are turned off in Fig.(2a), |Ψ(x)|≈0, whereas when they are both turned on in Fig.(2c), observe that |Ψ(x)|≈0.24 . Comparing Free field Fig. (2a) to potential on only Fig.(2b) @ x=40, illustrates the potential is the main reason the solution spreads out in x.

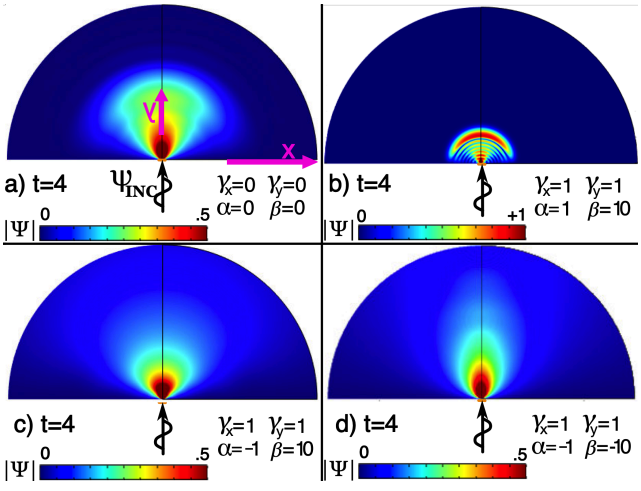

Figure 11 |Ψ | vs x,y for Linear vs Nonlinear 1 Slit Sol.

4.3.2 Ψ Pulse Solution :

The 1 slit |Ψ(x,y,t)| field solution, for a Fig.(1c) pulse type input, is shown in Fig.(12). The model parameters and geometry are exactly the same as Fig.(11).

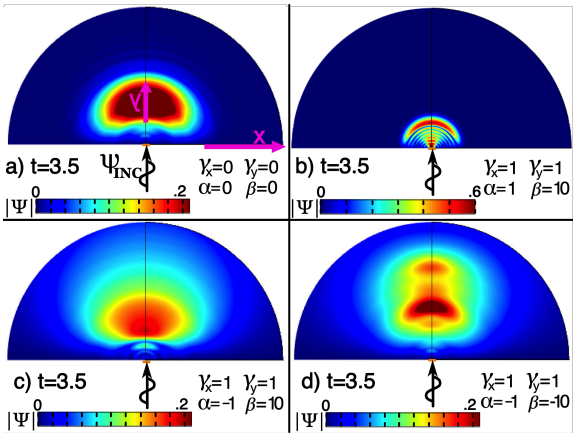

Figure 12 |Ψ | vs x,y for Pulse Input 1 Slit Solution

5. Concluding Remarks

COMSOL successfully solved the nonlinear Schrödinger equation (NLSE). There is good agreement between COMSOL and Mathematica FEM solutions for long 1-D models in PW waveguides. The 2-D models were run for both 1-slit and 2-slit configurations where classical |Ψ(x,y,t)| spoked alternating constructive and destructive interference patterns were experienced. Direct comparisons to the free field linear Schrödinger equation are made (i.e. V potential, β NL terms are zero) so that the effect of turning on the V and β terms are contrasted. Resolving the same 2-D models but thru only one slit, illustrates simplicity of |Ψ(x,y,t)| in the absence superimposing waves emanating from 2 slits. The local k-ω dispersion relation (holding local space coordinate x=x′ or r=r′) constant in the Ψ(x,y,t) PDE's { } multiplying coefficient) is a measure of the expected wave lengths for a given ω which is useful in a-priori selecting mesh sizes and also whether traveling waves can be supported in the locale of x=x′ or r=r′ .

6. References

[1] Kalinowski A.J. ,"Quantum Mechanics Applications Using the Time Dependent Schrödinger Equation …", COMSOL Conf. Proc. 2015.

[2] Bao W. "The Nonlinear Schrödinger Eq. and Applications in BEC and Plasma Physics", (IMS Lecture Notes, World Scientific)**9**, 2007,141-240) .

[3] Xavierc A. et al,"Computational Methods for the Dynamics of the Nonlinear Schrödinger Eq./ GPE", Computer Physics Comm. 00 (2013).